Monolithic TiO_2 with Controlled Multiscale Porosity via a Template-Free Sol−Gel Process Accompanied by Phase Separation

Junko Konishi,[†] Koji Fujita,*[,†] Kazuki Nakanishi,[‡] and Kazuyuki Hirao[†]

Department of Material Chemistry, Graduate School of Engineering, Kyoto University, Nishikyo-ku, Kyoto 615-8510, Japan, and Department of Chemistry, Graduate School of Science, Kyoto University, Kitashirakawa, Sakyo-ku, Kyoto 606-8502, Japan

Received July 26, 2006. Revised Manuscript Received September 22, 2006

This article describes the fabrication of multiscale porous nanocrystalline TiO_2 monoliths through a one-step method that combines a sol−gel process and phase separation in template-free conditions. A large-dimension monolith with well-defined macropores and a mesostructured anatase-type TiO_2 gel skeleton is spontaneously obtained by controlling the solution pH during the hydrolysis and polycondensation reactions of titanium alkoxides. The size of the macropores is adjusted by the starting composition, and a crystallized anatase TiO_2 skeleton is formed without heat treatment. The use of titanium alkoxide strengthens the gel network by the formation of chemical bonding in the condensation reaction, which yields porous monoliths with higher mechanical strength than for the case of porous monoliths derived from colloidal TiO_2 using freeze drying to maintain the porous morphology. The average crystallite size of anatase TiO_2 nanocrystals was found to be about 3.6 nm for the dried gel and about 5.0 nm for the gel calcined at 300 °C. As a result of the growth of the anatase TiO_2 nanoparticles, the mesopores with a median size of 5.0 nm are obtained. The high surface area (∼150 m^2/g) is maintained even after the heat treatment at 300 °C.

Introduction

Unique properties of titania (TiO_2) have been extensively exploited in diverse areas such as catalysis,[1] sensing,[2] electronics,[3] optics,[4] and separation science.[5] To extract a higher performance from TiO_2 with potential application, morphological control in a broad length scale ranging from nanometers to millimeters is required in addition to the compositional control in such ways as doping, solid solution, and organic−inorganic hybrid. In the subject of material design, multiscale porous materials have received a lot of attention because they offer multiple benefits arising from each pore size regime. For example, large pores such as macropores allow facile fluid transport, while the presence of additional mesopores gives rise to a large surface area that assists the contacts of fluid. In the research of porous TiO_2, various methods have been established to fabricate macroporous materials[4,6] and micro- or mesoporous materials,[7] and several synthetic strategies have been recently developed to form the bimodal porous structure. For instance, dual templating techniques using surfactants and latex spheres can produce TiO_2 powder with bimodal pore size distribution.[8] Recent reports have also demonstrated that macro-mesoporous structures can be prepared in the presence of a single surfactant[9] and even under a template-free condition.[10]

For several applications, simultaneous tailoring of the material shape (monolith, fiber, thin film, etc.) and the bimodal pore structure are important. For example, the presence of macropores ensures a high flow rate for liquid phases, while the mesopores can contribute to the separation of a mixture of molecules. Consequently, monolithic materials with multiscale porous structures find an application as a separation medium for high-performance liquid chromatography (HPLC);[11] monolithic HPLC columns, in which the porous monoliths are used as the stationary phase, allow much faster separation than the conventional ones packed with particles.[12] Thus, in separation science and many

* Corresponding author. E-mail: fujita@dipole7.kuic.kyoto-u.ac.jp. Tel.: +81-75-383-2432. Fax: +81-75-383-2420.
† Department of Material Chemistry, Graduate School of Engineering.
‡ Department of Chemistry, Graduate School of Science.

(1) Fujishima, A.; Honda, K. *Nature* **1972**, *238*, 37.
(2) Göpel, W.; Kirner, U.; Wiemhöfer, H. D.; Rocker, G. *Solid State Ionics* **1998**, *28*, 1423.
(3) O'Regan, B.; Grätzel, M. *Nature* **1991**, *353*, 737.
(4) Imfof, A.; Pine, D. J. *Nature* **1997**, *389*, 948.
(5) Buchmeiser, M. R. *J. Chromatogr., A* **2001**, *918*, 233.
(6) (a) Holland, B. T.; Blanford, C. F.; Do, T.; Stein, A. *Science* **1998**, *24*, 538. (b) Caruso, R. A.; Giersig, M.; Willig, F.; Antonietti, M. *Langmuir* **1998**, *14*, 6333.
(7) (a) Yang, P.; Zhao, D.; Margolese, D. I.; Chmelka, B. F.; Stucky, G. D. *Nature* **1998**, *396*, 152. (b) Wang, H.; Oey, C. C.; Djurišić, A. B.; Xie, M. H.; Leung, Y. H.; Man, K. K. Y.; Chan, W. K.; Pandey, A.; Nunzi, J. M.; Chui, P. C. *Appl. Phys. Lett.* **2005**, *87*, 023507.
(8) Holland, B. T.; Blanford, C. F.; Do T.; Stein, A. *Chem. Mater.* **1999**, *11*, 795.
(9) (a) Antonelli, D. M. *Microporous Mesoporous Mater.* **1999**, *33*, 209. (b) Yuan, Z.-Y.; Vantomme, A.; Léonard, A.; Su, B.-Li. *Chem. Commun.* **2003**, *13*, 1558. (c) Yuan, Z.-Y.; Ren, T. Z.; Su, B.-L. *Adv. Mater.* **2003**, *15*, 1462. (d) Deng, W.; Toepke, M. W.; Shanks, B. H. *Adv. Funct. Mater.* **2003**, *13*, 61. (e) Blin, J. L.; Léonard, A.; Yuan, Z.-Y.; Gigot, L.; Vantomme, A.; Cheetham, A. K.; Su, B.-L. *Angew. Chem., Int. Ed.* **2003**, *42*, 2872. (f) Carn, F.; Colin, A.; Achard, M.-F.; Deleuze, H.; Sanchez, C.; Backov, R. *Adv. Mater.* **2004**, *16*, 140. (g) Morris, M. A.; Reidy, H. M. *Ceram. Inter.* **2005**, *31*, 929.
(10) Collins, A.; Carriazo, D.; Davis, S. A.; Mann, S. *Chem. Commun.* **2004**, *5*, 568.
(11) Nakanishi, K. *J. Porous Mater.* **1997**, *4*, 67.
(12) (a) Tanaka, N.; Kobayashi, H.; Nakanishi, K.; Minakuchi, H.; Ishizuka, N. *Anal. Chem.* **2001**, *73*, 420A. (b) Svec, F., Tennikova, T., Deyl, Z., Eds. *Monolithic Materials: Preparation, Principles and Applications*; Journal of Chromatography Library 67; Elsevier: Amsterdam, 2003.

10.1021/cm0617485 CCC: $33.50
Published on Web 11/15/2006

environmental applications that include filters and photocatalysis, there is a strong need for the development of innovative techniques that would allow well-controlled synthesis of monolithic TiO_2 with multiscale porosity. Only limited synthesis techniques have been reported to meet such requirements.[13]

A sol−gel method accompanied by phase separation is one of the promising techniques for fabricating monolithic materials with a bimodal pore structure.[11] Well-defined macroporous silica (SiO_2)-based gels can be prepared by inducing phase separation parallel to the sol−gel transition. Subsequent solvent exchange of the macroporous gel with a basic aqueous solution produces mesopores with diameters of 5−10 nm via a process known as Ostwald ripening.[14] If the reliable and reproducible method can be applied to TiO_2 systems, the resultant TiO_2 monoliths will be useful for molecular separation in the field of biochemistry due to the ability of TiO_2 to selectively adsorb phosphorylated molecules such as peptides and proteins.[15] Unfortunately, the preparation of a multiscale porous TiO_2 monolith via the phase separation route has not been achieved in alkoxy-derived systems so far, since the high reactivity of titanium alkoxides makes it hard to control the structural development in the course of the hydrolysis and polycondensation.[16] Especially in the synthesis of the monolith, the difficulty becomes serious because highly reactive precursor has to be used in the concentrated condition. Thus, the preparation of TiO_2 monoliths with a bimodal pore size distribution still remains a challenging task, irrespective of the drastic progress in the synthesis of SiO_2-based monoliths including inorganic−organic hybrid SiO_2.[17]

In our previous study, "colloidal titania" was used as the TiO_2 source to circumvent the high reactivity of titanium alkoxide;[18] however, we had faced the problem related to the weak bonding strength between physically aggregated colloidal particles, an additional freeze-drying process was indispensable for maintaining the macroporous morphology, and the resultant dried gels broke apart easily.

In this paper, we describe a method for the fabrication of TiO_2 monoliths with multiscale porous structure from titanium "alkoxy-derived" sol−gel systems under template-free conditions. The desired pore structure is achieved by controlling the hydrolysis and polycondensation reactions. Starting from a homogeneous mixture of components under a strongly acidic condition, the gradual increase in solution pH induces the polycondensation reaction and enables the fabrication of large-size TiO_2 monoliths. A monolithic body with well-defined interconnected macropores is formed by the concurrent phase separation and sol−gel transition induced by the polymerization reaction, whereas micro- or mesopores are embedded in the interconnected gel skeleton comprised of nanocrystalline anatase TiO_2. A characteristic feature is the spontaneous formation of multiscale porous structure in a closed condition at a constant temperature, which obviates the need for any templating agents. Another feature is that the size and porosity of macropores can be tailored by selecting the starting compositions. Furthermore, the present alkoxy-derived method removes the necessity for the freeze-drying process, owing to the formation of strong chemical bonding through the condensation reaction. Namely, high mechanical strength can be accomplished in alkoxy-derived sol−gel systems, which allows the fabrication of large-dimension monoliths. Several benefits are expected to arise not only from the dual pore structure integrated in robust monoliths but also from the unique functions of TiO_2.

Experimental Section

Material Synthesis. Monolithic TiO_2 gels were prepared from the starting solution containing titanium *n*-propoxide ($Ti(O^nPr)_4$, Aldrich), hydrochloric acid (HCl, Hayashi Pure Chemical Ind., Ltd.), formamide (FA, Wako Pure Chemicals Ind., Ltd.), and water (H_2O). All chemicals were used as received without further purification. The molar ratio of the starting composition was $Ti(O^nPr)_4$/HCl/FA/H_2O = 1:0.5:0.5:*f*, where f = 20.50, 20.75, 21.00, 21.25, and 21.50. The gel preparation is as follows. Appropriate amounts of HCl, H_2O, and FA were added to $Ti(O^nPr)_4$ while stirring under an ice-cooled condition. After stirring for 5 min, the homogeneous solution was poured into a test tube and allowed to gel at 30 °C. The resultant wet gel was aged at 30 or 60 °C for 24 h and evaporation-dried at 60 °C for 7 days. Some of the dried gels were heat-treated at various temperatures between 300 and 700 °C for 3 h in air.

Measurements. The morphology of dried and heat-treated gels was observed by scanning electron microscopy (SEM; S-2600N, Hitachi, Ltd., Japan, with Pt coating) and field-emission scanning electron microscopy (FE-SEM; JSM-6700F, JEOL, Ltd., without coating). The size distribution of macropores was determined by mercury porosimetry (PORESIZER-9320, Micromeritics Co., U.S.A.). The mesoporous structure was characterized by a nitrogen adsorption−desorption isotherm (Tristar, Micromeritics Co., U.S.A.). The size distribution of the mesopore was calculated from the adsorption branch of the isotherm using the Barrett-Joyner-Halenda (BJH) method, and the surface area was obtained by the Brunauer-Emmett-Teller (BET) method.

X-ray diffraction (XRD) patterns were recorded on X-ray diffractometer (RINT2500, Rigaku, Japan) with Cu Kα radiation. The measurements were made on the powder specimens prepared by grinding monolithic gels. The size of crystallites was calculated from the full width at half-maximum of (101) diffraction peaks ascribed to the anatase phase using Scherrer's equation.

In order to evaluate the mechanical strength of dried and heat-treated gels, uniaxial compression tests were performed using compressive tester (CATY-500BL, Yonekura, Japan) so that the compressive fracture was determined. The measurements were made on monolithic circular cylinders of gels with flat smooth parallel cylinder faces and lengths between 5 and 10 mm. The samples were set on a plate and compressed by another plate. Fracture stress was determined as the stress at which visible cracks appeared in the sample. It should be noted that because the breaking point could

(13) (a) Carn, F.; Colin, A.; Achard, M.-F.; Deleuze, H.; Sanchez, C.; Backov, R. *Adv. Mater.* **2005**, *17*, 62. (b) Toberer, E. S.; Seshadri, R. *Adv. Mater.* **2005**, *17*, 2244.
(14) Iler, R. K. *The Chemistry of Silica, Solubility, Polymerization, Colloids and Surface Properties, and Biochemistry*; Wiley-Interscience: New York, 1979.
(15) (a) Pinkse, M. W. H.; Uitto, P. M.; Hilhorst, M. J.; Ooms, B.; Heck, A. J. R. *Anal. Chem.* **2004**, *76*, 3935. (b) Sono, A.; Nakamura, H. *Anal. Sci.* **2004**, *20*, 861.
(16) Livage, J.; Henry, M.; Sanchez, C. *Prog. Solid State Chem.* **1988**, *18*, 259
(17) (a) Amatani, T.; Nakanishi, K.; Hirao, K.; Kodaira, T. *Chem. Mater.* **2005**, *17*, 2114. (b) Brandhuber, D.; Torma, V.; Raab, C.; Peterlik, H.; Kulak, A.; Hüsing, N. *Chem. Mater.* **2005**, *17*, 4262.
(18) (a) Fujita, K.; Konishi, J.; Nakanishi, K.; Hirao, K. *Appl. Phys. Lett.* **2004**, *85*, 5595. (b) Konishi, J.; Fujita, K.; Nakanishi, K.; Hirao, K. *Chem. Mater.* **2005**, *18*, 864.

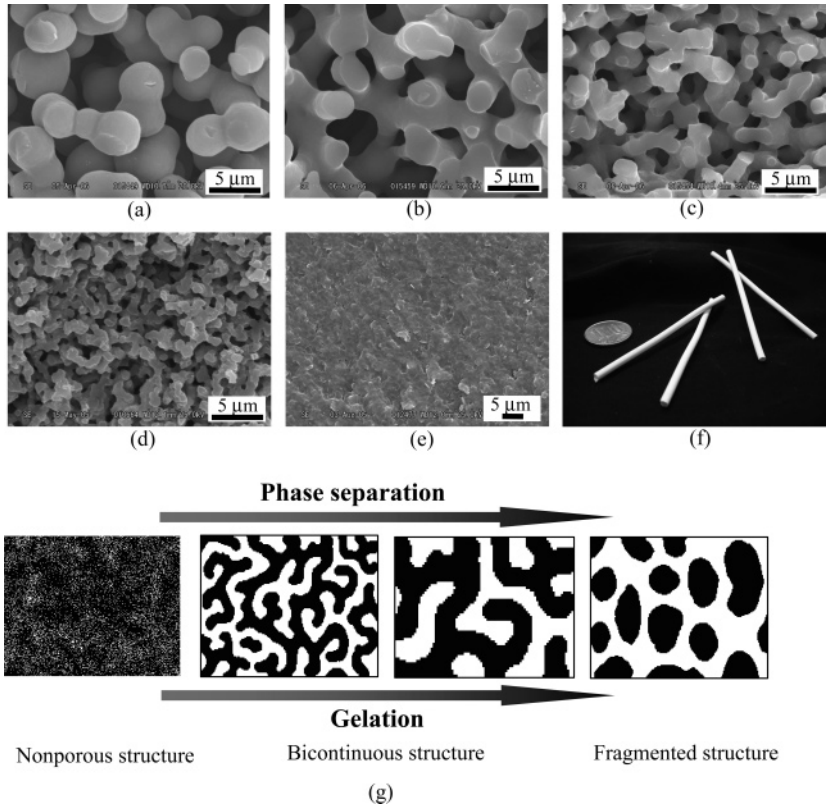

Figure 1. (a−e) SEM images of dried TiO_2 gels prepared with varied molar ratios of water/TiO_2, (a) $f = 20.50$, (b) $f = 20.75$, (c) $f = 21.00$, (d) $f = 21.25$, and (e) $f = 21.50$. (f) Digital picture of monolithic TiO2 gels prepared in Teflon tubes and a coin. (g) Schematic illustration of coarsening of phase-separated domains. Bicontinuous structure is obtained by inducing the phase separation in parallel to the gelation.

not be precisely detected as a result of compressive deformation, the data included some uncertainties.

Results and Discussion

Figure 1a−e shows SEM images of dried TiO_2 gels prepared with $f = 20.50$, 20.75, 21.00, 21.25, and 21.50, respectively. The gel prepared with $f = 20.50$ exhibits the morphology of particle aggregates, while that with $f = 21.50$ shows nonporous structure in the micrometer range. Well-defined bicontinuous macropores are clearly observed in the compositional range between $f = 20.75$ and 21.25. Careful design of the synthesis described below made it possible to synthesize the materials with controlled macroporous bicontinuous morphology. The first key point is the use of $Ti(O^nPr)_4$ as TiO_2 precursor to reduce the reactivity of polycondensation. $Ti(O^nPr)_4$-derived system ($f = 21.0$) exhibited substantially long gelation time (∼90 min), while the substitution of titanium isopropoxide $Ti(O^iPr)_4$ for $Ti(O^nPr)_4$ led to gelation instantly after the addition of H_2O in the preparation of starting solution. The second key point is the use of HCl as the strong acid catalyst, which also helps to reduce the reactivity of $Ti(O^nPr)_4$ to H_2O. In such a strongly acidic condition, the alkoxy groups in $Ti(O^nPr)_4$ are protonated to make their local charge more positive. The protonated alkoxy groups are in turn dissociated to enhance hydrolysis.[15] In comparison to hydrolysis, protonated hydroxy groups in the hydrolyzed species hinder the nucleophilic attack toward positively charged Ti ions, which retards the polycondensation reaction. In addition, alkoxy-derived oligomers grown by successive condensation are positively charged and stabilized by the electrostatic repulsion in the acid condition, because the solution pH is much lower than the isoelectric point of TiO_2, or pH = 5.5−6.0.[19] Thus, the use of HCl provides us with an opportunity to control the structural development in the polycondensation stage. The third important point is the use of FA which enables the control over the polycondensation rate and also effectively induces phase separation. FA is a highly polar solvent with hydrogen bonding and is hydrolyzed to produce ammonia in the presence of a strong acid. As a result of the hydrolysis of FA, the solution pH becomes higher in the polycondensation stage of TiO_2 oligomers. In the present case, the solution pH is below 0 immediately after mixing the starting solution and gradually increases to around 5 after 24 h. The gradual increase in pH accelerates the polycondensation reaction and eventually induces the sol−gel transition. At the same time, the polycondensation decreases the polarity of gel phase gradually by consuming the hydroxy groups, while the polarity of the solvent remains high. In the course of polycondensation, therefore, the phase separation is driven by the reduction of miscibility between the polar solvent and polycondensed inorganic species. A bicontinuous structure, in which both the separated phases are highly continuous and interconnected, is obtained when the phase separation is induced parallel to the sol−gel transition. On drying, the gel phase becomes the mesoporous skeleton, and the solvent phase turns into macropores. The variation of gel morphology with f as shown in Figure 1a−e can be explained in terms

(19) (a) Kallay, N.; Zalac, S.; Stefanic, G. *Langmuir* **1993**, *9*, 3457. (b) Rodriguez, R.; Blesa, M. A.; Regazzoni, A. E. *J. Colloid Interface Sci.* **1996**, *177*, 122.

Table 1. Shringkage and Fracture Stress of Alkoxy- and Colloid-Derived TiO_2 Gels with Interconnected Macropores (Diameter $\sim 1\ \mu m$)

sample[a]	condition[b]	diameter[c] (mm)	fracture stress[d] (MPa)
alkoxy-derived TiO_2 gels	as-dried	11	5.3×10^2
	heat-treated at 300 °C	7.8	4.0×10^3
colloid-derived TiO_2 gels	as-dried	9.0	5.5
	heat-treated at 300 °C	9.0	3.7

[a] Alkoxy- and colloid-derived TiO_2 monolithic gels were prepared in Teflon tubes with diameter ϕ 17 mm and ϕ 9 mm, respectively. [b] Alkoxy-derived gel was evaporation-dried at 60 °C, while colloid-derived gel was freeze-dried to keep the macroporous morphology.[18] After drying, both the gels were heat-treated at 300 °C. [c] Diameter of parallel faces of circular-cylinder-shaped gels. [d] Stress that generates visible cracks in the compression test.

of a change in phase-separation tendency as mentioned below.

Here, it should be mentioned that the problem relevant to the high reactivity of titanium alkoxides can be alleviated if a stabilized dispersion of colloidal TiO_2 is used as the starting material. We recently developed a method to fabricate macro-mesoporous TiO_2 monoliths by the sol−gel process using an aqueous colloidal TiO_2 as a starting material,[17] although a freeze-drying process was required to maintain the porous structure after the gelation; simple evaporation drying in air spoiled the porous structure. Even if the porous structure was held after freeze-drying, the resultant dried gel was fragile because the network consisted of physically weak aggregates of colloidal TiO_2 particles, which limits the application in diverse areas. Our approach described here, that is, the fabrication of TiO_2 monoliths via the alkoxy-derived sol−gel route, overcomes this obstacle by the formation of strong chemical bonding through the hydrolysis and polycondensation reaction. The difference in connectivity of the gel network between alkoxy- and colloid-derived gels manifests itself in the physical properties such as mechanical strength. In order to evaluate the mechanical properties of gels with interconnected macroproes (diameter $\sim 1\ \mu m$), we carried out uniaxial compression tests so that the compressive fracture stress could be determined. The alkoxy- and colloid-derived gels employed in the compressive test were prepared in Teflon tubes with ϕ 17 mm and ϕ 9 mm, respectively. After gelation at 30 °C, both the gels were aged at 60 °C. The compressive fracture stress evaluated for dried and heat-treated gels shaped into circular cylinders is summarized in Table 1, together with the diameters of parallel cylinder faces. For alkoxy-derived gels, the diameter is decreased to 11 mm upon evaporation drying and further reduced to 7.8 mm upon heat treatment, while the interconnected macroporous morphology is maintained. The shrinkage is caused not only by the capillary force originated from solvent evaporation but also by the condensation of titanium species with unreacted alkoxy or hydroxy groups. The fracture stress of alkoxy-derived dried gel is larger compared to that of colloid-derived dried gel and is significantly enhanced by heat treatment at temperatures as low as 300 °C. These results indicate that even after gelation, unreacted alkoxy or hydroxy groups condense with each other during aging, drying, and heat

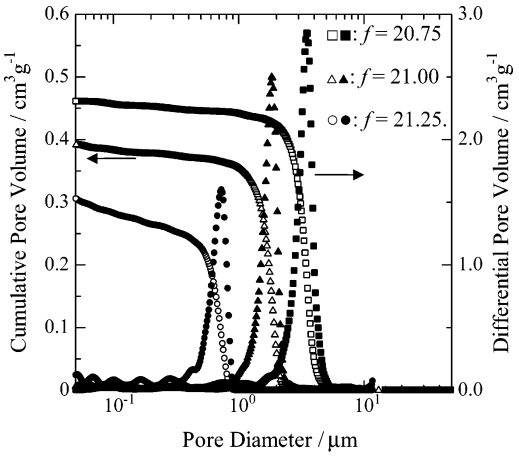

Figure 2. Pore size distribution of the dried TiO_2 gels measured by the mercury intrusion method. (□, ■) $f = 20.75$, (△, ▲) $f = 21.00$, and (○, ●) $f = 21.25$.

treatment, producing the robust gels. For colloid-derived gels, on the contrary, no shrinkage is recognized during aging, freeze-drying, and heat treatment, and the fracture stress is less susceptible to heat treatment. These results imply that after gelation, the particle aggregates comprising the interconnected skeleton do not form almost any chemical bonding with each other, leading to the fragile gels. Thus, it is reasonable to conclude that the formation of chemical bonding though the condensation in alkoxy-derived systems is responsible for the high mechanical integrity. The ability of producing robust TiO_2 gels without the need for a freeze-drying process could make the present synthesis more versatile and feasible, which would bring a great advantage in practical applications.

Using the present technique, well-defined macroporous TiO_2 gel monoliths are spontaneously formed in a closed condition. The interconnected gel skeleton and macroporous channel spread in space homogeneously into every corner of the resultant gel. Thus, a TiO_2 monolith with a desired shape and size can be fabricated simply by pouring the starting solution into an appropriate mold. Figure 1f shows a digital image of products prepared in Teflon tubes, demonstrating the feasibility of processing in different molds including the confined space such as a capillary.

The size of the macropores can be controlled by adjusting the timing of the onset of phase separation relative to the sol−gel transition, because the domain formation during the phase separation involves a coarsening process as schematically illustrated in Figure 1g. The control over the pore size is readily accomplished through only the change in the starting composition. Pore size distributions measured by Hg porosimetry are shown in Figure 2 for dried gels having bicontinuous structure. The macropores are sharply distributed, and the pore size decreases with the increasing amount of H_2O in the starting composition [see also Figure 1b−d]. The variation of pore size with the amount of H_2O may be explained in terms of the compatibility between the polar solvent and the TiO_2 phase. In the system with a larger amount of H_2O, the hydrolysis reaction of titanium alkoxide is more strongly promoted to increase the number of hydroxyl groups on the surface of the TiO_2 oligomers. Therefore, the compatibility of the two phases increases in

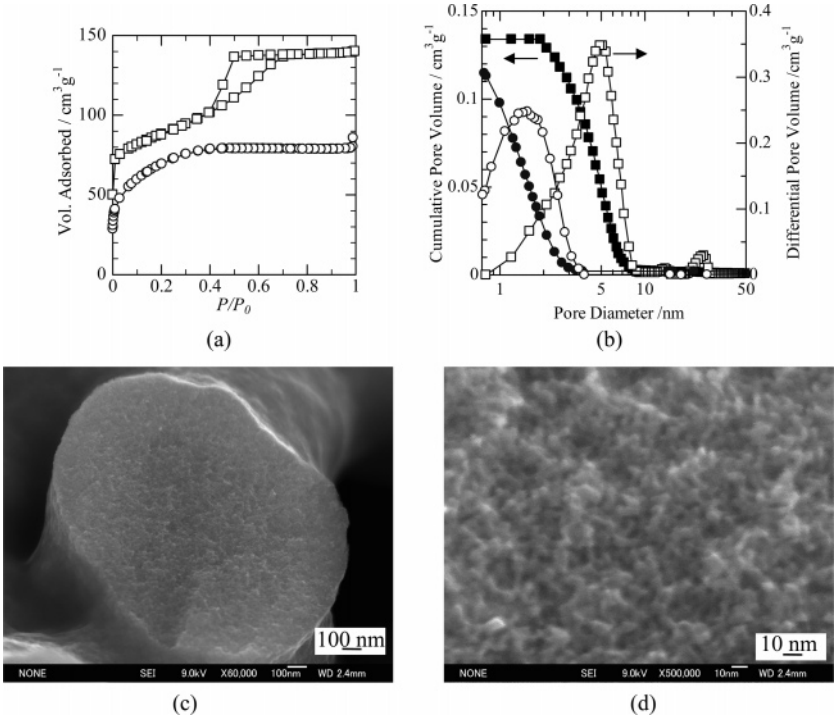

Figure 3. Mesoscale characterizations of the TiO_2 gels prepared with $f = 21.00$: (a) nitrogen adsorption−desorption isotherm of the dried gel (○) and the gel heat-treated at 300 °C (□). Curve of the gel heat-treated at 300 °C is shifted upward by 50 cm^3 g^{-1} for clarity. (b) Pore size distribution of the dried gel (○, ●) and the gel heat-treated at 300 °C (□, ■). (c) FE-SEM image of the gel heat-treated at 300 °C. (d) Higher magnification image of part c.

the order of $f = 20.75 < f = 21.00 < f = 21.25$. Thus, as the amount of H_2O is increased, the phase-separation tendency becomes weaker, and the finer bicontinuous structure is obtained as a result of the later onset of phase separation, the smaller pores being left behind after evaporation drying. Further increase in the amount of H_2O ($f >$ 21.25) makes the phase-separation tendency too weak, so the resultant gels are nonporous in the micrometer range due to a much later onset of the phase separation relative to the gelation [Figure 1e]. On the contrary, when the amount of H_2O is smaller ($f < 20.75$), the phase separation takes place much earlier than the gelation, and the bicontinuous structure fragments into spherical particles to reduce the interfacial energy [Figure 1a].

For the purpose of characterizing the mesoporous structures, N_2 adsorption−desorption isotherms were measured on the dried gel and the gel heat-treated at 300 °C ($f =$ 21.00). The result is shown in Figure 3a; Figure 3b is the corresponding BJH pore size distribution. The dried gel shows a type-I isotherm according to IUPAC classification, which indicates the existence of micropores smaller than 2 nm. The BJH pore size distribution curve is centered at about 1.4 nm. This situation is greatly different from the case of TiO_2 gels derived from colloids,[18] where the mesopores with a broad size distribution (20−50 nm) are embedded into the macroporous framework due to the physical aggregation of colloidal TiO_2. In the case of the present alkoxy-based process, the framework with considerably fine mesh is obtained as a result of the homogeneous polycondensation of TiO_2 oligomers. In addition, the condensation reaction of unreacted hydroxyl groups continues during aging and drying even after the bicontinuous structure is fixed by the gelation, which makes the gel network robust enough to endure the collapse of porous structure during solvent evaporation in air.

By heat treatment at 300 °C, the adsorption−desorption hysteresis loop changes into a type-H2 isotherm. The BJH pore size distribution curve is centered at about 5.0 nm, which agrees with the FE-SEM observation [Figure 3c,d]. Obviously, the heat treatment at 300 °C brings about the growth of TiO_2 nanoparticles to produce the accessible mesostructure. The specific surface area is calculated to be about 150 m^2 g^{-1} using the BET method.

Figure 4a displays XRD patterns of the dried gel and those heat-treated at various temperatures ($f = 21.00$). The XRD pattern for the dried gel reveals that nanocrystalline anatase TiO_2 is obtained from the alkoxy-derived systems. The appearance of anatase-type crystals without heat treatment is one of the significant advantages, since most alkoxy-derived sol−gel processes produce an amorphous phase (the crystalline TiO_2 powders are well-known to be produced only under limited dilute conditions). The production of the crystalline phase instead of the amorphous phase is related presumably to a nearly complete hydrolysis of the alkoxide and slower kinetics of the subsequent condensation reaction. When titanium alkoxide is dissolved in an acidic aqueous solution, the coordination number of the titanium ion increases from 4 to 6. This is because the empty *d* orbitals of titanium ions accept oxygen lone pairs of water molecules to induce the coordination expansion. After the almost complete hydrolysis, the 6-fold structural units undergo the slow condensation through corner and edge sharing, leading to the formation of anatase TiO_2 crystal. Even if amorphous aggregates are formed with a loose binding, the structural rearrangement into a more stable crystalline phase, that is,

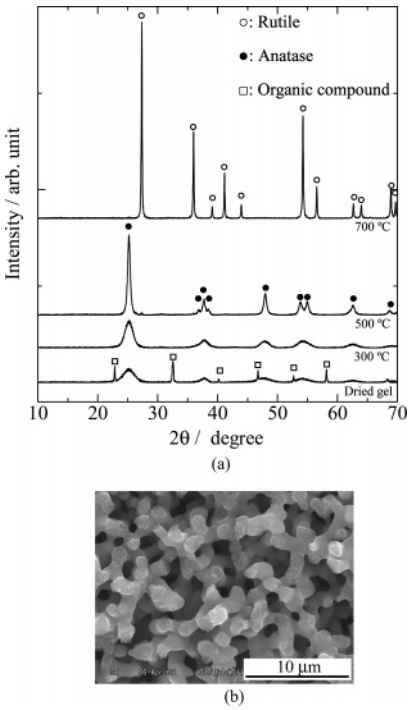

Figure 4. (a) XRD patterns of TiO_2 gels heat-treated at various temperatures ($f = 21.00$). Symbols ○, ●, and □ represent diffraction peaks ascribed to the anatase and rutile phases and the organic compound, respectively. (b) SEM image of titania gel heat-treated at 700 °C ($f = 21.00$). The micrometer-range morphology of the dried gel prepared from the same starting composition is shown in Figure 1c.

anatase TiO_2, easily occurs in the acidic condition because the titanium oxo or hydroxo bridges are broken to enhance the dissolution and reprecipitation.[20] The XRD pattern of dried gel also exhibits sharp diffraction peaks at around $2\theta = 23$, 32, 40, 47, 52, and 58°. These diffraction peaks, which are associated with organic species, disappear almost completely during the heat treatment at 300 °C. On the other hand, the diffraction peaks ascribed to anatase TiO_2 become narrower and more intense at elevated calcination temperatures. As calculated from Scherrer's equation using an anatase (101) diffraction peak at around $2\theta = 25$ °, the average crystallite size is found to be about 3.6 nm for the dried gel and about 5.0 nm for the gel heat-treated at 300 °C. Heating at temperatures higher than 700 °C converts the anatase phase into the rutile phase without spoiling the macroporous morphology [Figure 4b].

Examination on the separation efficiency of biomolecules utilizing the TiO_2 monolith with multiscale porous structures has gained interest and is now in progress to demonstrate the possibility of the application of TiO_2 monoliths to HPLC devices. Future work will be dedicated toward the formation of well-defined mesopores with controlled geometry.

Conclusion

TiO_2 monoliths with multiscale porous structures have been successfully prepared by using $Ti(O^nPr)_4$ as the precursor. The use of HCl as the strongly acidic catalyst allows us to control the hydrolysis and polycondensation reaction of $Ti(O^nPr)_4$, while the polycondensation reaction is controlled by the pH increase through the hydrolysis of FA. Polymerization-induced phase separation leads to the formation of well-defined bicontinuous macropores. The pore size can be tailored by adjusting the starting compositions. The interconnected gel skeleton consists of an assembly of anatase-type TiO_2 nanocrystals without heat treatment. The formation of multiscale porous structure proceeds spontaneously in a closed condition, which enables the fabrication of TiO_2 monoliths into different shapes in the appropriate molds. Heating at 300 °C produces 5-nm-sized mesopores due to the growth of nanoparticles, while maintaining the macroporous morphology.

Acknowledgment. We appreciate Dr. Takeshi Shiono for help with compression tests and Prof. Himanshu Jain for helpful discussions. This study was partly supported by the Industrial Technology Research Grant Program (04A25023) and Grant for Practical Application of University R&D Results under the Matching Fund Method from New Energy and Industrial Technology Development Organization (NEDO), Japan, and also by the Grant-in-Aid for Scientific Research (18360316) from the Ministry of Education, Culture, Sports, Science, and Technology (MEXT), Japan. J.K. thanks the Grant-in-Aid for Fellow (No. 17•2224) from Japan Society of the Promotion Science (JSPS).

CM0617485

(20) (a) Gopel, M.; Chan, W. J. M.; Jonghe, L. C. D. *J. Mater. Sci.* **1997**, *32*, 6001. (b) So, W. W.; Park, S. B.; Moon, S. J. *J. Mater. Sci. Lett.* **1998**, *17*, 1219.